Secondary Peak Detection of PPG Signal for Continuous Cuffless Arterial Blood Pressure Measurement

Xiaochuan He, Rafik A. Goubran, *Fellow, IEEE*, and Xiaoping P. Liu, *Senior Member, IEEE*

***Abstract*— The arterial blood pressure (ABP) is one of the most important physiological parameters for health monitoring. Most of the blood measurement devices in the market determine the ABP through the inflation and the deflation of a cuff controlled by a bladder. This method is very uncomfortable for most of the users and may even cause anxiety, which in turn can affect the blood pressure (BP) (white coat syndrome). This paper investigates a cuffless nonintrusive approach to estimate the BP. The main idea is to measure the pulse transit time (PTT), i.e., the delay between the R-peak of the electrocardiogram (ECG) signal and the following peak of the finger photoplethysmograph (PPG) signal. The main problem of this approach is that when the dicrotic notch of the PPG signal is unobservable, the position and the amplitude of the main peak of the PPG signal will be changed. As a result, the correlation between the BP and the PTT can be affected. To overcome this problem, three types of secondary peak detection methods are designed to reveal the secondary peak from the original PPG signal. Actual ECG, PPG, and the BP measurements extracted from the Multiparameter Intelligent Monitoring in Intensive Care II database that contains clinical signal data reflecting real measurements are used. The results verify that the proposed detection methods improve the correlation relationship between the BP and the PTT, and demonstrate that the adjusted PTT can be used as an indicator of the ABP by removing the dicrotic notch impact on the PPG signal.**

***Index Terms*— Arterial blood pressure (ABP), dicrotic notch, finger photoplethysmogragh (PPG) signal, Gaussian curve fitting (GCF), pulse transit time (PTT).**

I. Introduction

THE RISK of having arteriosclerosis and hypertension is no longer just for old-aged patients. The age of the patients with various cardiovascular diseases is pointing to much younger groups and the number of people who need daily monitoring of cardiovascular health risks is significantly increased [1]. On the other hand, the tension on the utilization of public resources in hospitals is becoming more and more serious. So, the type of healthcare is tending to individual-centered other than hospital-centered [2]. The patients also want to be as independent as possible as they are aging. Hence, the need of self-monitoring devices dramatically increases in the recent decades and the techniques to make individual measurement more comfortable and convenient are required and developed.

Arterial blood pressure (BP) is highly related to cardiovascular conditions and is an efficient way to detect cardiovascular diseases [3]–[6]. As we know, the most precise way to obtain the ABP is using invasive measurement, in which a catheter is inserted into the patients' vessel [7]. However, this measurement has a high demand on the doctor's or nurse's operation skills and the patients' conditions, not to mention the pain and potential risk to the patient.

Nowadays, nonintrusive and noninvasive detective methods are becoming the basic requirements for wearable medical devices, in particular, when the devices are to be used by patients for self-monitoring without the assistance from the physicians or nurses [8], [9]. Instead of using the conventional cuff [10], [11], there have been several studies on measuring blood pressure (BP) noninvasively and continuously, such as arterial tonometry, column clamp method, and pulse transit time (PTT). For arterial tonometry, an array of pressure sensors was pressed against the skin over an artery [12]. With the volume-clamp method, the finger arterial pressure was measured by a finger cuff and an inflatable bladder combined with an infrared plethysmogram, which consists of an infrared light detector and light source [13]. It is also demonstrated that the BP can be obtained by measuring the pulse wave velocity (PWV) [14]. However, the measurement of the PWV is a very challenging task since it needs different models, mathematical calculations, accurate measurement of the blood flow, and a thorough analysis. Fortunately, the PTT has been proved to be a very useful tool to describe the relationship between the PWV and BP [15], [16].

The correlation between the BP and the PTT has been studied in quite a few research papers [17]–[19]. Some signal acquisition medical devices presented in these papers introduced significant delays between different types of biomedical signals [20]. This will apparently affect the observation results. In [21], linear regression was used to estimate the BP, which led to an estimation error up to 25 mmHg. A parameter from photoplethysmograph (PPG) dicrotic notch, called as relative amplitude of secondary peak (RAS), was used for the

Manuscript received July 7, 2013; revised October 31, 2013; accepted November 6, 2013. Date of publication January 27, 2014; date of current version May 8, 2014. This work was supported in part by the Natural Sciences and Engineering Research Council and in part by the Industrial and Government Partners through the Healthcare support through Information Technology Enhancements Strategic Research Network. The Associate Editor coordinating the review process was Dr. Domenico Grimaldi.

The authors are with the Department of Systems and Computer Engineering, Carleton University, Ottawa, ON K1S 5B6, Canada (e-mail: xche@sce.carleton.ca; goubran@sce.carleton.ca; xpliu@sce.carleton.ca).

Color versions of one or more of the figures in this paper are available online at http://ieeexplore.ieee.org.

Digital Object Identifier 10.1109/TIM.2014.2299524

estimation of systolic BP (SBP) in [22]. The result showed that the underestimated bias could be largely reduced by introducing the RAS. Baek *et al.* [23] proposed a method of BP estimation using multiple regression with pulse arrival time and two other confounding factors, heart rate and Time_deri_b, which was the duration from the maximum derivation point to the maximum of dicrotic notch in the PPG signal.

This paper continues our previous research on the evaluation of the correlation between the BP and PTT [24]. Since there have been a great number of researches demonstrating that the dicrotic notch of the PPG is quite useful for the BP estimation, we extend our work to the detection of the secondary peak of the PPG signal. Usually, there are two main peaks in one period of the PPG signal. Between of the two peaks is what is known as dicrotic notch. Sometimes the dicrotic notch cannot be easily observed in some PPG signals, which means the secondary peak may be embedded into the main peak because of the characteristics of the signal, e.g., the two waves are too close to each other, the amplitude of the secondary peak is too small compared with the main peak, or the span of the secondary peak is not big enough to be noticed from the main wave. In addition to the invisibility of the useful feature parameters, one serious problem caused is that the nonexistence of the secondary peak will impact the position and the amplitude of the main peak of the original PPG signal. This will further impact the time difference between the R-peak of the electrocardiogram (ECG) signal and the main peak of the following PPG signal, which is the PTT. Then the PTT can no longer be regarded as a secure estimation parameter to measure corresponding ABP.

In this paper, three detection methods are proposed: 1) symmetrical curve fitting (SCF) method; 2) Gaussian curve fitting (GCF) method; and 3) adaptive curve fitting (ACF) method. The ABP, ECG, and PPG signals are extracted from the Multiparameter Intelligent Monitoring in Intensive Care (MIMIC) II database, where the synchronization of all types of signals can be guaranteed. The correlation values between the SBP and the adjusted PTT is calculated based on the fitted data points. In addition, linear, quadric, and cubic regression curves for the BP and the adjusted PTT are depicted.

The structure of this paper is organized as follows. The background of this paper is briefly introduced in Section I. In Section II, the signals used with the three secondary peak detection methods and the processing procedure are depicted. The correlation between the BP and PPG signal and the polynomial regression of the simulation data are illustrated in Section III. The discussions are given and conclusions are drawn in Section IV.

II. Methodology

A. MIMIC II Database

The MIMIC II database contains clinical signals and vital signs time series obtained from hospital medical information systems. The signals in the MIMIC II database are multiparameter recordings, which are obtained from both a bedside monitor and the medical records of the patient [25]. Clinical data were obtained from the CareVue Clinical Information System (models M2331A and M1215A; Philips Healthcare, Andover, MA) as well as from hospital electronic archives [26]. So, the measurement instrumentation used to acquire the biomedical signals in this paper is real clinical devices and the method we proposed is not only working on some specified cases, but also for most of the clinical cases. In order to verify that the adjusted PTT and the SBP have high correlation and to reduce the interference of other issues, the data points used for the simulations are selected from the neat portions of the patient's record. So, the signals are clean enough for detecting the feature points. The tool used to extract the signals from the database is called PhysioBank ATM, which has several toolboxes, including plotting the waveforms of one specific signal, showing samples as text, and exporting signals as .mat [27].

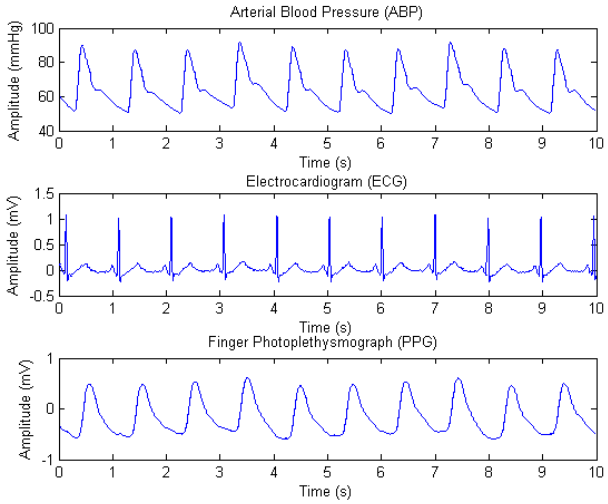

Fig. 1. Pure ABP, ECG, and PPG signals extracted from the MIMIC database.

In this paper, a hundred individual records are extracted for simulations. These records include synchronized ABP, ECG, and finger PPG signal. Each record contains $\sim$ 10 segments, and each segment lasts 10 s and has an average of 10 cycles, shown in Fig. 1. By obtaining the data in this way, the range of the SBP and diastolic BP (DBP) for each patient can cover from $<$80 to $>$150 mmHg and from $<$60 to $>$110 mmHg, respectively. The ECG signals are recorded at 125 sampling frequency and with eight to 12-bit resolution.

B. Feature Parameters

The PTT defined in this paper is the time from the R-peak of the ECG signal to the following finger PPG peak. Some features of the ECG signal are hard to be detected, in particular, when there is noise existing in the signal. So, instead of detecting the inconspicuous features of the ECG signal, R-peak is easier to be observed due to its unique shape, and is more stable than the other wave peaks.

Fig. 2 shows the feature parameters employed for the BP estimation. The red curve, blue curve, and green curve represent the BP, finger PPG, and ECG signal, respectively. The R-peak index is determined by locating the local maxima of each ECG cycle. The SBP is calculated based on the maximum points of the BP. The dicrotic notch of the PPG

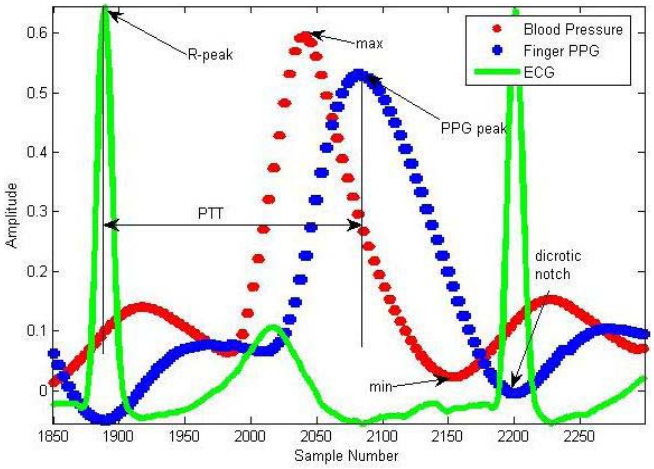

Fig. 2. Feature points and PTT determined from one set of synchronous ECG and finger PPG signals used for BP estimation.

signal is obvious in Fig. 2. However, not all the dicrotic notches of the PPG signal is visible from the database.

C. Signal Processing and Data Analysis

As mentioned in the previous paper [24], the processing procedure of this paper involves several steps and can be described as follows.

Step 1: Select the neat and complete signal segments that have the specific BP range.

Step 2: Denoise the extracted signal segments.

Step 3: If there is only one visible main peak of the PPG signal, apply secondary peak detection methods on the original PPG signal to visualize the secondary peak of the PPG. The procedure of the three different detection methods will be described in the following part. If there are two main peaks in one period of PPG signal, continue to step 4.

Step 4: Detect the peaks of R-wave of ECG signal and the peaks of the PPG signal.

Step 5: Detect the maximum and minimum extremes of the BP signal.

Step 6: Determine the delay of each corresponding R-peak and adjusted PPG peak, which is the adjusted PTT.

Step 7: Calculate the correlation value of the SBP versus adjusted PTT for each record and draw the linear, quadric, and cubic regression curves.

Step 8: Compare the fitted regression curves and select the best one for future estimation.

The main peak of the PPG signal happens when blood is pumped from the heart and the secondary peak of the PPG signal is caused by the reflection of the blood in the vessel. When the reflection is not strong enough, the secondary peak will be buried and the dicrotic notch will become unobservable. The three types of methods to reveal the secondary peak of the PPG signal are: 1) SCF method; 2) GCF method; and 3) ACF method.

1) SCF Method: The purpose of the SCF method is to trailoff the amplitude of the main peak of the PPG signal and then to observe the secondary peak. The steps of the SCF method are as follows.

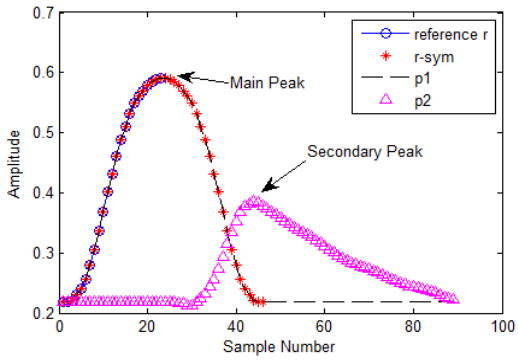

Fig. 3. Feature waveforms of SCF method.

Step 1: The upstroke side in the main peak of the PPG signal mainly depends on the heartbeat. This part of the PPG signal is firstly selected as the reference r.

Step 2: Find the axial symmetry of the reference curve regarded as r_sym. Integrate r and r_sym together to form the first peak signal noted as $p1$. Pad $p1$ to the same length as the original PPG signal.

Step 3: Subtract the padded $p1$ from the original PPG signal and obtain the residue $p2$, whose main peak is the secondary peak of the PPG signal.

In order to make the procedure of the SCF method easier to be read, we added Fig. 3 to show the different steps of the SCF method.

Fig. 3 shows the feature waveforms in different procedure steps of the SCF method. The blue circle graph represents the reference curve r. The red asterisk line is the axial symmetry of r. The black dash and the pink triangular line stand for the $p1$ and $p2$, respectively.

The position of the main peak of the adjusted PPG signal is the same as the original signal, because the SCF method is the first method we proposed to detect the secondary peak and the effect of of the dicrotic notch to the PTT has not been considered. The simulation results in Section III will show the improvement of the correlation between the BP and the adjusted PTT with the concern of the position shifting, which indicates the importance of the visibility of the secondary peak of the PPG signal in the BP estimation.

2) GCF Method: GCF method is another way to separate the secondary peak from the main peak. Suppose the baseline of the fitting curve is at y_0 and the curve is not tilted, the Gaussian equation used only involves three parameters: the amplitude A, the mean μ, and the standard deviation σ [28]. The equation is normally expressed as

$$y = y_0 + Ae^{-(x-\mu)^2/2\sigma^2}. \tag{1}$$

One of the most important steps in applying the GCF is to find the three parameters A, μ, and σ of the Gaussian curve, which can best fit the data points of the original PPG signals. μ is the center of the fitted curve and σ controls the width of the curve.

The procedure of the GCF method is as follows.

Step 1: Obtain the PPG signal from the database and look into the shape of the signal. If no dicrotic notch can be detected, the GCF method needs to be employed.

Step 2: Calculate the second derivative of the PPG signal, plot it, and observe the zero crossing points of the second derivative curve.

Step 3: Assuming the zero crossing points around the peak of the PPG signal are x_1 and x_2, the position and the standard deviation of the fitted Gaussian curve can be estimated using the following equations: $x = (x_1 + x_2)/2$ and $\sigma = |x_1 - x_2|/2$. The amplitude of the Gaussian curve A is calibrated by the amplitude of the main wave of the PPG signal.

Step 4: Subtract the first Gaussian curve from the original PPG signal and get the secondary peak signal.

The purpose of applying the zero crossing points of the second derivative of PPG is to reduce the calculation complexity of the whole procedure. Basically, the principle of the GCF method is to find the Gaussian curve that best fits the upstroke side of the original PPG signal. By finding the best fitted Gaussian curve, it means to locate the mean and the standard deviation of the fitted curve. Instead of using exhaustion method from observation, we decide to use the zero crossing points of the second derivative curve as a secondary means to reduce the search range and the calculation complexity. So even when there is disturbing noise, the position of the zero crossing points may be changed, but this will not affect it to locate the position of the fitted Gaussian curve.

3) ACF Method: Based on the performance of the SCF method and the GCF method, an adaptive GCF method is designed to detect the secondary peak from the PPG signal. The fitting curve of the ACF method is a Gaussian curve and the procedure of the adaptive method is as follows.

Step 1: Obtain the PPG signal and look into the shape of the signal. If no dicrotic notch can be detected, an adaptive GCF method needs to be employed.

Step 2: Adapt the mean and the standard deviation positions based on the position of the main peak and the shape of the upstroke of the main peak.

Step 3: Adjust the amplitude of the fitting curve A to 80% of the main peak.

Step 4: Subtract the fitting curve from the original PPG signal to get the secondary peak of the PPG signal.

D. Correlation

To evaluate the strength and the direction of the relationship between the ABP and the adjusted PTT signal, the correlation r and R^2 are applied. Since the adjusted PTT is decreasing with the increasing of the BP, the correlation between these two signals should be negative. The formula to calculate the correlation r between two sets of data points is as

$$r = \frac{\sum xy - \sum x \sum y/n}{\sqrt{\left[\sum x^2 - \frac{(\sum x)^2}{n}\right]\left[\sum y^2 - \frac{(\sum y)^2}{n}\right]}} \tag{2}$$

where x and y represent the BP data points and the adjusted PPG data points, respectively. n is the length of the data and the value of r supposed to be in the range from -1 to 0.

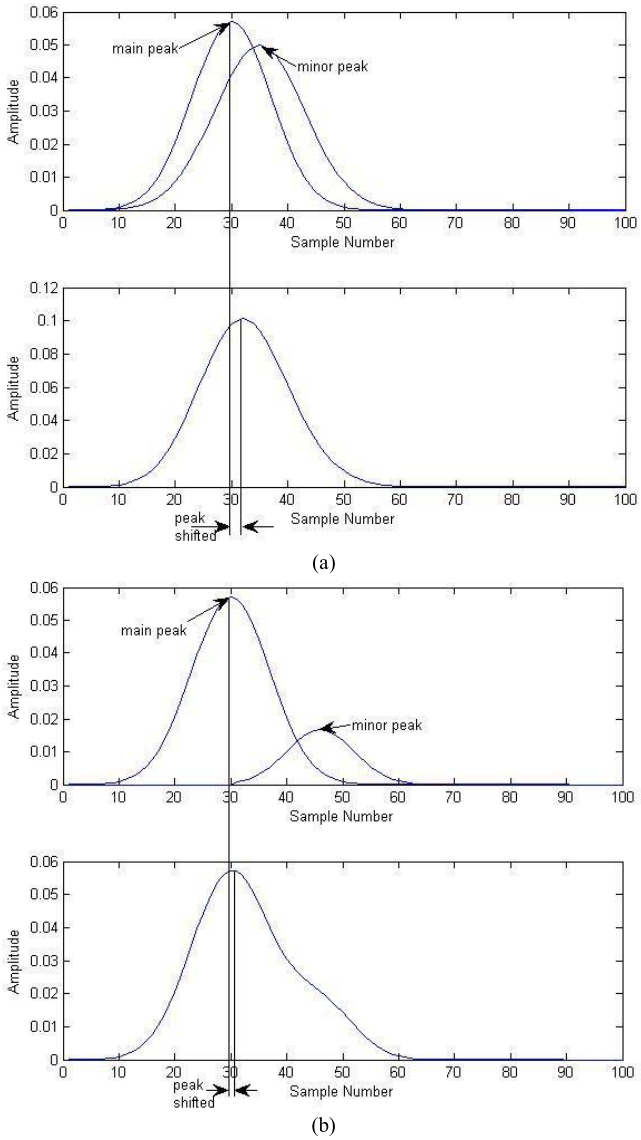

Fig. 4. Peak shifting phenomenon caused by the combination of two Gaussian curves. (a) Scenario I: two curves are too close to each other. (b) Scenario II: the difference of the amplitude of the two curves is too large.

When r is smaller than -0.8, it can be determined that the two sets of data points have strong correlation.

The correlation r is only suitable for linear regression, R^2 can be used to evaluate both linear and nonlinear regression. R^2 provides information about the goodness of the regression curve in fitting the model.

III. Simulations and Result

The simulations of this paper are taken on 100 patients, 65 being male and 35 female, aging from 60 to 80 years. The data points are extracted from the MIMIC II database. The synchronism of the ABP signal, ECG signal, and PPG signal for each record are guaranteed.

A. Peak Shifting Phenomenon

To show the importance of this paper, the peak shifting phenomenon is briefly depicted in this part. Taking Gaussian

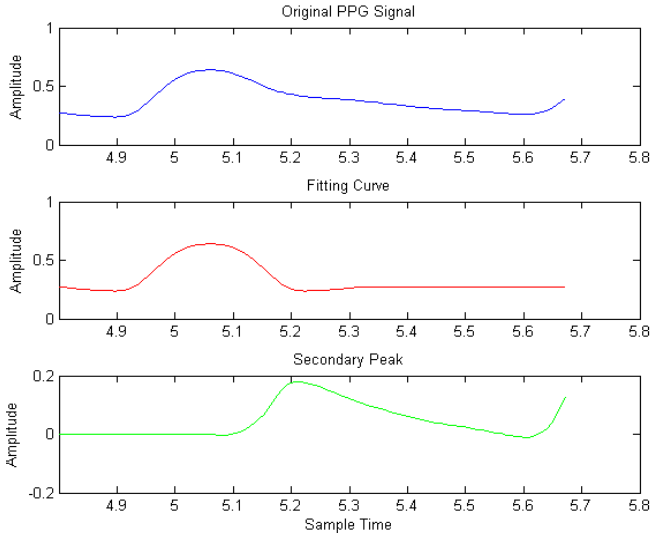

Fig. 5. Secondary peak detection procedure of SCF method.

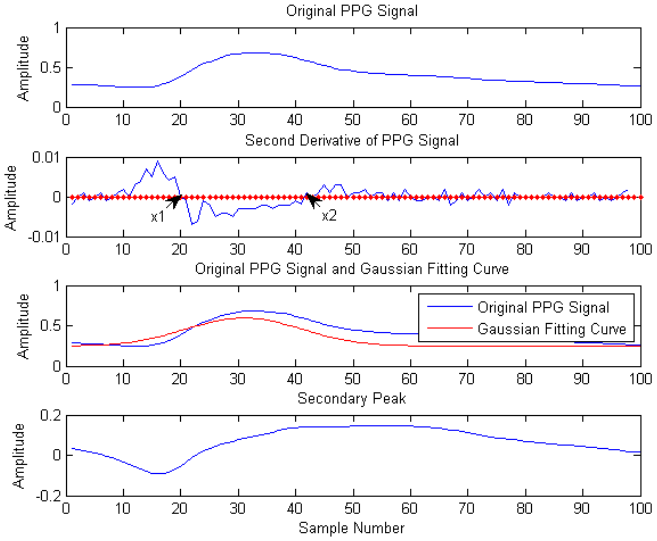

Fig. 6. Secondary peak detection procedure of GCF method.

curves as an example, Fig. 4 shows two of the many scenarios that the main peak shifts and the minor peak become invisible after combing the two curves together.

The situation of Fig. 4(a) is two curves that are too close to each other and Fig. 4(b) shows the scenario that the difference of the amplitude of the two curves is too large. If we define the peak with greater amplitude as the main peak and the peak with smaller amplitude as the minor peak, under both conditions it is obvious that the position of the main peak has been shifted to right and the minor peak disappears.

B. Secondary Peak Detection

Three types of secondary peak detection methods are proposed in this paper: SCF, GCF, and ACF. One patient (No. 3302802 in MIMIC II database) without visible secondary peak of the PPG signal is chosen to show the detection procedure of the three methods.

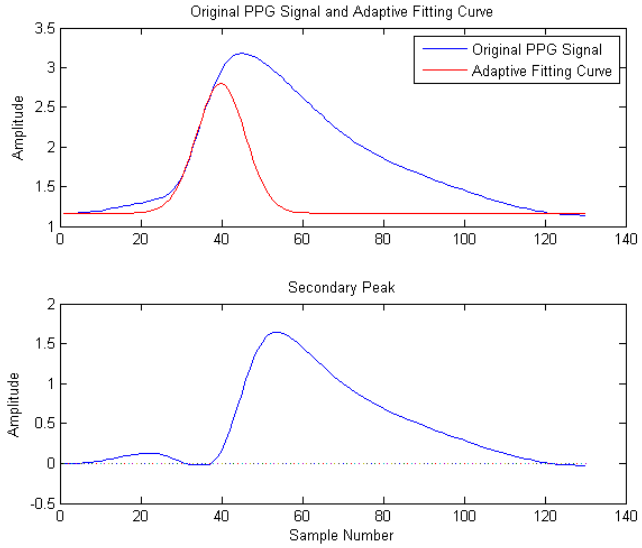

Fig. 7. Secondary peak detection procedure of ACF method.

Fig. 5 shows the detection procedure of the SCF method. The blue curve, red curve, and green curve represent the original PPG, the fitting curve, and the secondary peak detected from the original PPG signal, respectively. The SCF method is the first method we tested for visualizing the secondary peak of the PPG. The peak shifting phenomenon is not considered, so the position of the peak of the fitting curve is the same as the peak of the original signal.

In Fig. 6, the GCF method is employed to detect the secondary peak of the PPG. The second figure shows the second derivative of the PPG signal with the zero crossing points of the second derivative curve used to calculate the position and the standard deviation of the Gaussian fitting curve. Applying the value of $x1$ and $x2$ obtained from the second plot, the Gaussian fitting curve is determined as the red curve shown in the third plot and the secondary peak of the PPG signal is shown in the fourth plot. We can observe that there is a concave segment in the secondary peak due to the amplitude difference between the original PPG signal and the Gaussian fitting curve.

Based on the SCF and GCF, the ACF method is developed for the secondary peak detection. In Fig. 7, the original PPG signal and the adaptive fitting curve are shown in the first plot. The value of the mean and the standard deviation of the fitting curve are adapted to fit the position and the upstroke side of the main peak. From the second plot, it is revealed that the disturbance of the secondary peak is much smaller than the other two methods and the peak shifting problem is clearly displayed.

C. Correlation With BP

Before showing the scatter plot and the regression models, the correlation between the adjusted PTT and the BP after applying our proposed secondary peak detection method is illustrated by the intuitive plots, providing the information about the peak shifting phenomenon and the time delay

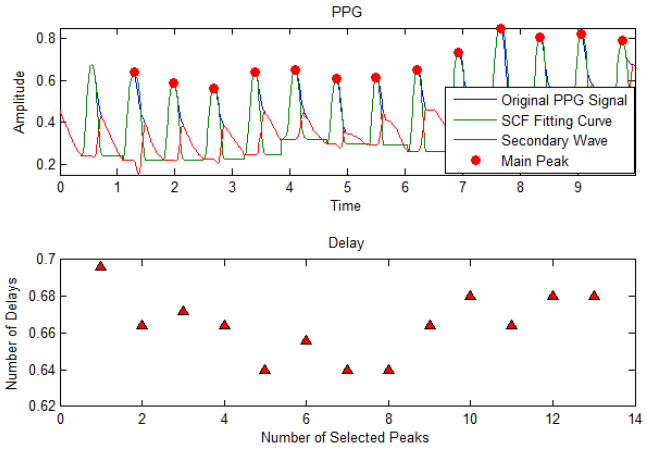

Fig. 8. Adjusted PPG signal and adjusted PTT by SCF.

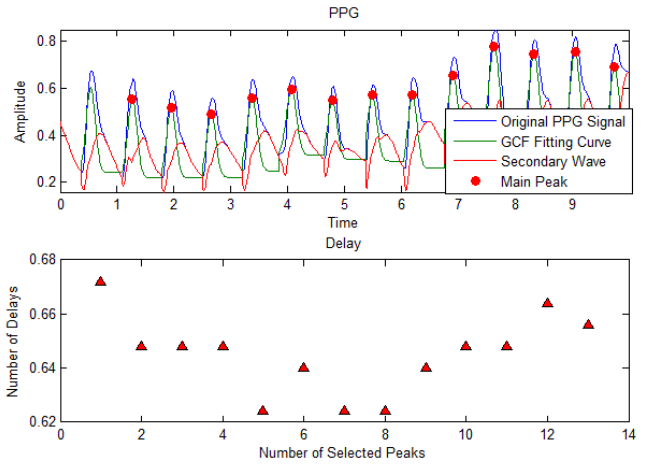

Fig. 9. Adjusted PPG signal and adjusted PTT by GCF.

between the R-peak of the ECG signal and the corresponding next following PTT signal.

The SBP and DBP for Figs. 8–10 are ∼120 and 60 mmHg, respectively. As mentioned before, the adjusted PTT for the SCF is actually the same as the PTT of the original PPG, which can be used to compare the performance of considering the peak shifting phenomenon. From the plots we can observe that the range of the delay after employing the GCF and the ACF is smaller than the original PTT, which demonstrates that the adjusted PTT is more specific for certain value of the BP.

Fig. 11 shows the R-squared values between the adjusted PTT signal and the BP when using different secondary peak detection methods. R-squared indicates how much the change in one variable can be explained by the change of the other variable, no matter their relationship is linear or nonlinear. It is obvious that the ACF has better performance than the SCF, which means the reduction of the peak shifting problem and the detection of the secondary wave of the PPG signal are very necessary and important in using the PTT for BP measurement.

Fig. 12 shows the scatter plot for the SBP versus adjusted PTT using different secondary peak detection methods and the linear (dashed line), quadric (dotted line), and cubic (solid line)

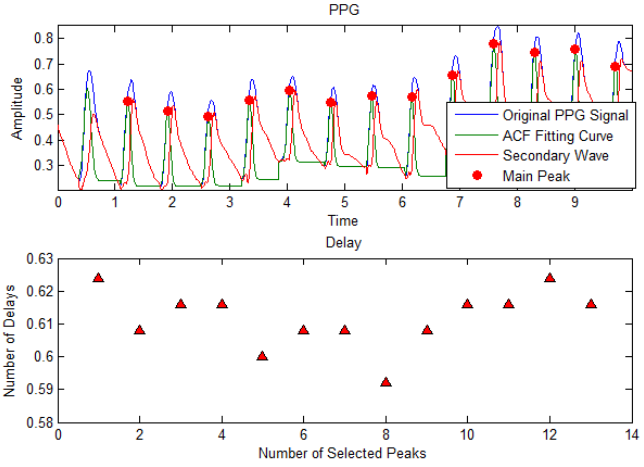

Fig. 10. Adjusted PPG signal and adjusted PTT by ACF.

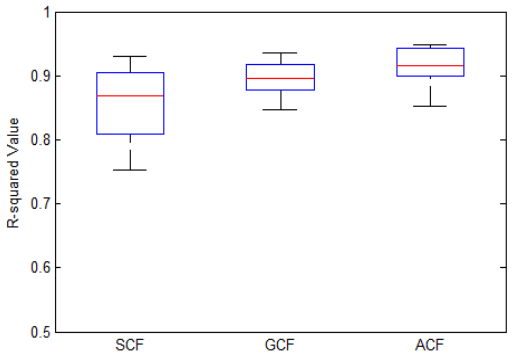

Fig. 11. R-squared values between the adjusted PTT and the BP using SCF, GCF, and ACF detection methods.

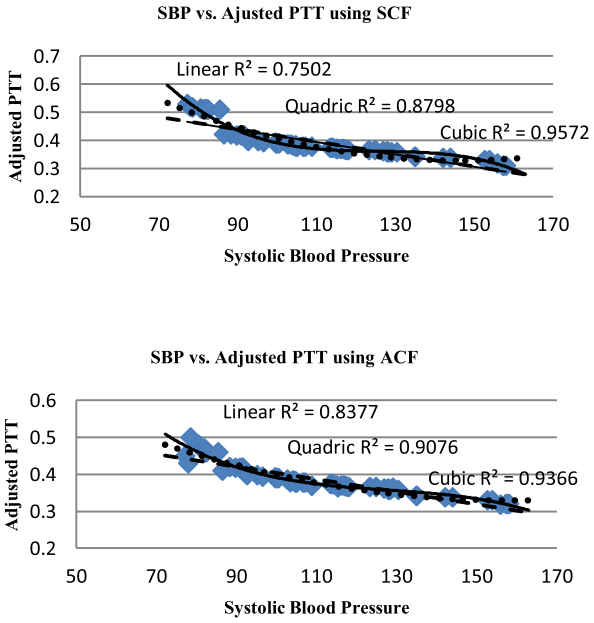

Fig. 12. Scatter plot for the SBP versus adjusted PTT and three regression curves.

regression curves. The curves and the R-square values show that the ACF detection method can provide better adjusted PTT, which has higher correlation with BP, in particular,

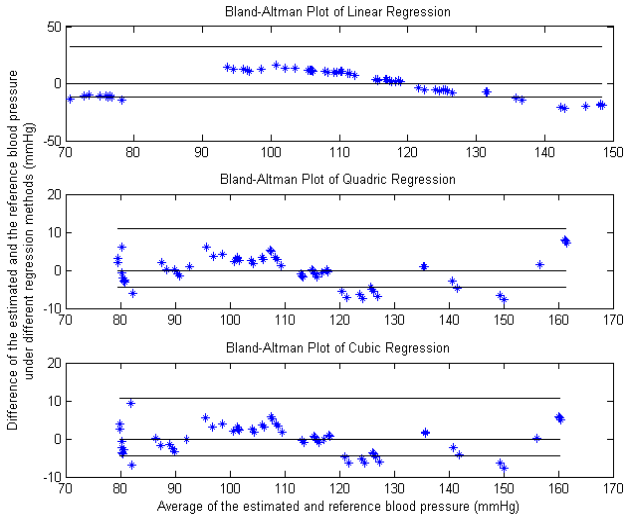

Fig. 13. Bland–Altman plot for the estimated and the reference BP under different regression methods.

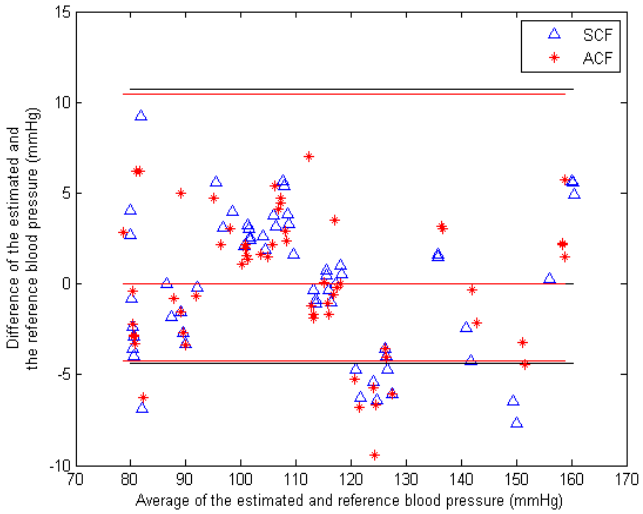

Fig. 14. Bland–Altman plot for the estimated and the reference BP by SCF and ACF methods.

TABLE I
ME AND STANDARD DEVIATION OF DIFFERENT SECONDARY WAVE DETECTION METHODS FOR PATIENT #3302802

Performance	SCF	GCF	ACF
ME(mmHg)	3.54	3.28	3.06
SDE(mmHg)	4.35	3.97	3.69

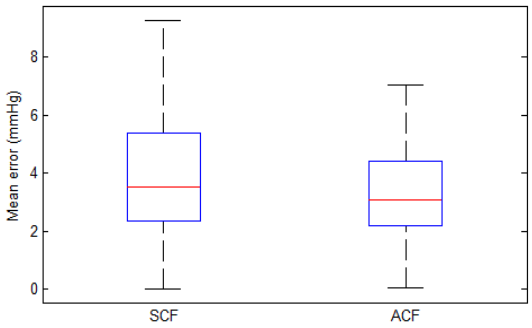

Fig. 15. Boxplot of the ME for the systolic BP estimation by SCF and ACF methods for patient #3302802.

when using linear regression model. In order to further illustrate the consistence between the proposed algorithm and the clinical data, Fig. 13 shows the Bland–Altman plots under different regression methods. With more times of regression calculation, the cubic regression model fits the data points better and the peak shifting impact will be further reduced.

The performance was depicted in terms of mean error (ME) and standard deviation of error (SDE). Since what we are trying to observe from the values is how close our estimation is to the measured BP, we are applying ME or mean absolute error as criteria. Table I lists in detail the values of the ME and SDE for different secondary wave detection algorithms. It can be observed from the table that the ACF method has smaller ME and SDE than the other two methods, which means the estimated BP obtained from the ACF has smaller bias and error variance.

Fig. 14 shows the Bland–Altman plot of the SBP estimation of the proposed methods versus the reference, which shows the agreement between predicted and reference BP on average. The blue triangular and the red asterisk represent the performance of the SCF and ACF methods, respectively. We can observe that the majority of the points locate within the limits of agreement. The curve obtained by the SCF method can predict the BP within 3.54 ± 4.35 mmHg of the reference, whereas for the ACF method, the value is 3.06 ± 3.69 mmHg. This demonstrates that the estimation of the BP can be improved by reducing the dicrotic notch impact and detecting the secondary wave of the PPG signal.

To better demonstrate how the secondary peak detection can improve the BP estimation results, Fig. 15 shows the boxplot of ME values of the SCF and ACF. In Fig. 15, the red central mark is the mean value of the error, the edges of the box are the 25th and 75th percentiles, and the black lines are the extreme points. We can observe that the ME of the SCF method can be as big as 9.27 mmHg, whereas the maximum value of ME of ACF method is 7.04 mmHg. The mean values of error for the SCF and ACF methods are 3.54 and 3.06 mmHg, respectively. In other words, the ACF is better than the SCF in both mean and variance of the errors.

The actual correlation between adjusted PTT and SBP should be higher than the results, since the signals used in the simulation were regarded as pure noise-free signals and no denoising processing was done before the extraction of the feature parameters.

IV. CONCLUSION

PTT is a commonly used parameter for ABP measurement. Usually, the PTT is defined as the time difference from the R-peak of the ECG signal to the next following main peak of the corresponding PPG signal. Sometimes the dicrotic notch or the secondary peak of the PPG signal is not visible, leading to the peak shifting of the main peak of the PPG signal, which will impact the accuracy of the PTT value. This problem is

very serious when the PTT is used for the BP estimation. In this paper, three types of secondary peak detection methods were developed, which were the SCF method, GCF method, and ACF method. Then the correlation between the adjusted PTT and the ABP was calculated. Linear regression, quadric regression, and cubic regression models were used to evaluate the relationship between the adjusted PTT and the SBP. Simultaneous BP, ECG, and PPG signals were extracted from the MIMIC II database. Simulation results demonstrated that the GCF and ACF could resolve the peak shifting problem and the adjusted PTT had higher correlation with the BP than the original PTT without observable dicrotic notch. Among the three regression models, the cubic regression method fitted the adjusted PTT versus BP data points the best. This investigation verified that the absence of the secondary peak of the PPG signal could impact the correlation between the PTT and BP. The proposed curve fitting method could reduce this impact and the adjusted PTT could be used to determine the BP continuously and noninvasively without the use of a cuff.

REFERENCES

[1] C. J. Murray, J. A. Lauer, R. C. Hutubessy, L. Niessen, N. Tomijima, A. Rodgers, *et al.*, "Effectiveness and costs of interventions to lower systolic blood pressure and cholesterol: A global and regional analysis on reduction of cardiovascular-disease risk," *The Lancet*, vol. 361, pp. 717–725, Mar. 2003.

[2] J. J. Rutherford, "Wearable technology," *IEEE Eng. Med. Biol. Mag.*, vol. 29, no. 1, pp. 19–24, May/Jun. 2010.

[3] S. Ahmad, M. Bolic, H. Dajani, V. Groza, I. Batkin, and S. Rajan, "Measurement of heart rate variability using an oscillometric blood pressure monitor," *IEEE Trans. Instrum. Meas.*, vol. 59, no. 10, pp. 2575–2590, Oct. 2010.

[4] P. Dupuis and C. Eugene, "Combined detection of respiratory and cardiac rhythm disorders by high-resolution differential cuff pressure measurement," *IEEE Trans. Instrum. Meas.*, vol. 49, no. 3, pp. 498–502, Jun. 2000.

[5] A. Silvani, D. Grimaldi, S. Vandi, G. Barletta, R. Vetrugno, F. Provini, *et al.*, "Sleep-dependent changes in the coupling between heart period and blood pressure in human subjects," *Amer. J. Physiol. Regulatory, Integrative Comparative Physiol.*, vol. 294, pp. 1686–1692, May 2008.

[6] S. Ahmad, S. Chen, K. Souerdan, I. Batkin, M. Bolic, H. Dajani, *et al.*, "A prototype of an integrated blood pressure and electrocardiogram device for multi-parameter physiologic monitoring," in *Proc. IEEE Conf. Instrum. Meas. Technol.*, May 2010, pp. 1244–1249.

[7] J. A. Kitterman, R. H. Phibbs, and W. H. Tooley, "Catheterization of umbilical vessels in newborn infants," *Pediatric Clin. North Amer.*, vol. 17, pp. 895–912, Nov. 1970.

[8] S. Saponara, M. Donati, T. Bacchillone, L. Fanucci, I. Sanchez-Tato, C. Carmona, *et al.*, "Remote monitoring of vital signs in patients with chronic heart failure: Sensor devices and data analysis perspective," in *Proc. IEEE Conf. SAS*, Feb. 2012, pp. 1–6.

[9] E. Balestrieri and S. Rapuano, "Instruments and methods for calibration of oscillometric blood pressure measurement devices," *IEEE Trans. Instrum. Meas.*, vol. 59, no. 9, pp. 2391–2404, Sep. 2010.

[10] T. Weber, S. Wassertheurer, M. Rammer, E. Maurer, B. Hametner, C. C. Mayer, *et al.*, "Validation of a brachial cuff-based method for estimating central systolic blood pressure," *Hypertension*, vol. 58, pp. 825–832, Nov. 2011.

[11] M. V. Moer and K. Barbe, "Influence of the cuff deflation mode on oscillometric blood pressure measurements," in *Proc. IEEE Int. Workshop Med. Meas. Appl.*, May 2011, pp. 652–656.

[12] E. A. Zorn, M. B. Wilson, J. J. Angel, J. Zanella, and B. S. Alpert, "Validation of an automated arterial tonometry monitor using association for the advancement of medical instrumentation standards," *Blood Pressure Monitor.*, vol. 2, pp. 185–188, Aug. 1997.

[13] K. Jagomagi, J. Talts, R. Raamat, and E. Lansimies, "Technical note: Continuous non-invasive measurement of mean blood pressure in fingers by volume-clamp and differential oscillometric method," *Clin. Physiol.*, vol. 16, pp. 551–560, Sep. 1996.

[14] Y. Miyauchi, S. Koyama, and H. Ishizawa, "Basic experiment of blood-pressure measurement which uses FBG sensors," in *Proc. IEEE Int. Conf. Instrum. Meas.*, May 2013, pp. 1767–1770.

[15] L. A. Geddes, M. H. Voelz, C. F. Babbs, J. D. Bourland, and W. A. Tacker, "Pulse transit time as an indicator of arterial blood pressure," *Psychophysiology*, vol. 18, pp. 71–74, Jan. 1981.

[16] E. Pinheiro, O. Postolache, and P. Girao, "Pulse arrival time and ballistocardiogram application to blood pressure variability estimation," in *Proc. IEEE Int. Workshop Med. Meas. Appl.*, May 2009, pp. 132–136.

[17] R. Shriram, A. Wakankar, N. Daimiwal, and D. Ramdasi, "Continuous cuffless blood pressure monitoring based on PTT," in *Proc. ICBBT*, Apr. 2010, pp. 51–55.

[18] G. Fortino and V. Giampa, "PPG-based methods for non-invasive and continuous blood pressure measurement: An overview and development issues in body sensor networks," in *Proc. IEEE Int. Workshop Med. Meas. Appl.*, Apr. 2010, pp. 10–13.

[19] M. Y. M. Wong, C. C. Y. Poon, and Y. T. Zhang, "An evaluation of the cuffless blood pressure estimation based on pulse transit time technique: A half year study on normotensive subjects," *Cardiovasc Eng.*, vol. 9, no. 1, pp. 32–38, Apr. 2009.

[20] J. Muehlsteff, X. L. Aubert, and M. Schuett, "Cuffless estimation of systolic blood pressure for short effort bicycle tests: The prominent role of the pre-ejection period," in *Proc. 28th Annu. Int. Conf. IEEE EMBC*, Aug. 2006, pp. 5088–5092.

[21] S. Deb, C. Nanda, D. Goswami, J. Mukhopadhyay, and S. Chakrabarti, "Cuff-less estimation of blood pressure using pulse transit time and pre-ejection period," in *Proc. Int. Conf. Converg. Inf. Technol.*, Nov. 2007, pp. 941–944.

[22] W. B. Gu, C. C. Y. Poon, and Y. T. Zhang, "A novel parameter from PPG dicrotic notch for estimation of systolic blood pressure using pulse transit time," in *Proc. ISSS-MDBS*, Jun. 2008, pp. 86–88.

[23] H. J. Baek, K. K. Kim, J. S. Kim, B. Lee, and K. S. Park, "Enhancing the estimation of blood pressure using pulse transit time and two confounding factors," *Physiol. Meas.*, vol. 31, no. 2, pp. 145–157, 2010.

[24] X. He, R. A. Goubran, and X. P. Liu, "Evaluation of the correlation between blood pressure and pulse transit time," in *Proc. IEEE Int. Workshop Med. Meas. Appl.*, May 2013, pp. 17–20.

[25] (2012, Jul.). *MIMIC II: Waveform Database Overview* [Online]. Available: http://physionet.org/mimic2/mimic2_waveform_overview.shtml

[26] M. Saeed, M. Villarroel, A. T. Reisner, G. Clifford, L. W. Lehman, G. Moody, *et al.*, "Multiparameter intelligent monitoring in intensive care II (MIMIC-II): A public-access intensive care unit database," *Crit Care Med.*, vol. 39, pp. 952–960, May 2011.

[27] (2012, Jul.). *The Physioband ATM Toolbox* [Online]. Available: http://www.physionet.org/cgi-bin/ATM

[28] A. Goshtasby and W. D. O'Neill, "Curve fitting by a sum of Gaussians," *Graph. Models Image Process.*, vol. 56, pp. 281–288, Jul. 1994.

Xiaochuan He received the B.Sc. and M.Sc. degrees in biomedical engineering from Shandong University, Jinan, China, in 2006 and 2009, respectively. She is currently pursuing the Ph.D. degree in electrical engineering from Carleton University, Ottawa, ON, Canada.

Her current research interests include biomedical signal processing, nonintrusive biological signal measurement, and adaptive filter theory.

Rafik A. Goubran (M'87–SM'08–F'12) received the B.Sc. and M.Sc. degrees in electrical engineering from Cairo University, Cairo, Egypt, in 1978 and 1981, respectively, and the Ph.D. degree in electrical engineering from Carleton University, Ottawa, ON, Canada, in 1987.

He joined the Department of Systems and Computer Engineering in 1987. He was a Chair of the same department from 1997 to 2006 and is currently the Dean of the Faculty of Engineering and Design, Carleton University. He was a Research Scientist with the Elisabeth Bruyere Research Institute, Ottawa. He was involved in several research projects with industry and government organizations in the areas of digital signal processing, biomedical engineering, sensors, data analytics, microphone arrays, and the design of smart independent living environments for seniors.

Dr. Goubran is the Founding Director of the Ottawa-Carleton Institute for Biomedical Engineering, and a member of the Association of Professional Engineers of Ontario.

Xiaoping P. Liu (M'02–SM'07) received the Ph.D. degree from the University of Alberta, Edmonton, AB, Canada, in 2002.

He has been with the Department of Systems and Computer Engineering, Carleton University, Ottawa, ON, Canada, since 2002, and is currently a Professor. He has published more than 200 research articles.

Dr. Liu serves as an Associate Editor for several journals, including the IEEE ACCESS, the IEEE/ASME TRANSACTIONS ON MECHATRONICS, and the IEEE TRANSACTIONS ON AUTOMATION SCIENCE AND ENGINEERING. He received the 2007 Carleton Research Achievement Award, the 2006 Province of Ontario Early Researcher Award, the 2006 Carty Research Fellowship, the Best Conference Paper Award of the 2006 IEEE International Conference on Mechatronics and Automation, and the 2003 Province of Ontario Distinguished Researcher Award. He is a Licensed Member of the Professional Engineers of Ontario.